OPTIMIZATION OF A TBA WITH STABLE OPTICS AND MINIMAL LONGITUDINAL DISPERSION AND CSR-INDUCED EMITTANCE GROWTH[*]

Chengyi Zhang[†][1], Yi Jiao[1], Key Laboratory of Particle Acceleration Physics and Technology,
Institute of High Energy Physics, Chinese Academy of Sciences, 100049 Beijing, China
Cheng-Ying Tsai, Department of Electrotechnical Theory and Advanced Electromagnetic Technology,
Huazhong University of Science and Technology, 430074 Wuhan, China
[1]also at University of Chinese Academy of Sciences, 100049 Beijing, China

Abstract

In the beam transfer line which often consists of dipoles to deflect the beam trajectory, longitudinal dispersion effect and emission of coherent synchrotron radiation (CSR) will lead to beam phase space distortion, thus degrading the machine performance. In this study, optimizations of a triple-bend achromat (TBA) cell are conducted using the multi-objective particle swarm optimization (MOPSO) method to suppress the CSR-induced emittance growth and minimize the longitudinal dispersion functions up to high orders, simultaneously. For the longitudinal dispersion function, results of three optimization settings are reported, which makes the TBA design first-order, second-order, and higher-order isochronous. Furthermore, we study the shortest possible beamline length of the higher-order isochronous TBA design, which may pave the way to designing a more compact beam transfer line.

INTRODUCTION

In modern high-brightness electron accelerators, preserving the beam quality from the source has long been pursued. However, in a beam transfer line, which may consist of bending magnets, the performance of a high-brightness electron beam may be degraded by the coherent synchrotron radiation (CSR) and the residual longitudinal dispersion. CSR can have a significant impact on the beam dynamics both transversely and longitudinally. In the transverse plane, it causes energy deviation and brings about dilution of the transverse emittance in the dispersive bending system [1]. In the longitudinal plane, CSR effect can give rise to the microbunching instability (MBI) [2–7].

In addition, the longitudinal dispersion effect can also influence the longitudinal dynamics, since in the dipole magnet, the particle's momentum deviation δ is correlated to the longitudinal bunch coordinate z via R_{56}, T_{566}, U_{5666}, etc., which are often referred to as the longitudinal dispersion functions [8]. The transfer map for the longitudinal coordinate from the beam line entrance (denoted with subscript i)

to the exit (denoted with subscript f) can be expressed as

$$z_f = z_i + R_{56}\delta_i + T_{566}\delta_i^2 + U_{5666}\delta_i^3 + O\left(\delta_i^4\right). \quad (1)$$

This kind of correlation causes deviation of the final longitudinal position from the center of the bunch. For the free-electron laser (FEL) beams with an energy chirp (i.e., $dE/(E\,dz)$), this correlation may result in undesirable bunch length variation. This kind of $z - \delta$ correlation may become rather severe for bunches with large δ, e.g., at FEL saturation leading to synchrotron sideband instability [9]. Thus in the beam transfer line design, it is of vital importance to mitigate the CSR effect and the longitudinal dispersion effect *simultaneously* in order to maintain high beam quality. Although the additional energy deviation caused by CSR is unavoidable, the CSR-induced emittance growth and the longitudinal dispersion functions, i.e., R_{56}, T_{566}, U_{5666}, etc., could be minimized.

In this study, a simple TBA cell is designed with practical considerations (e.g., quadrupoles and sextupoles are added for dispersion matching and chromaticity correction, respectively), as shown in Fig. 1.
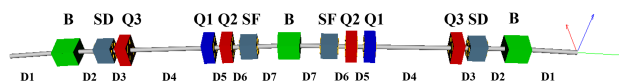

Figure 1: The lattice structure of TBA design and the magnet layout. The green cuboids represent dipoles, the red ones and the blue ones represent focusing quadrupoles and defocusing quadrupoles, respectively, while the indigo blue ones represent sextupoles.

MOPSO OPTIMIZATION AND RESULTS

The MOPSO [10] method is adopted in our optimization, which is suitable to handle multi-objective optimization problems and has been widely used in accelerator optimization problems (see, e.g., [11–14]).

In our design, the parameters of dipole magnet is fixed, i.e., $L_B = 0.4$ m, = 4°. The center-symmetric structure with three identical dipoles provides a 12-degree horizontal bending. The quadrupoles are grouped into three different families, one family of which is used for dispersion matching. Moreover, two families of sextupoles are used to correct the chromaticity. There are eight free variables, among which

six are the drift lengths and the remaining two variables are the strengths of the quadrupoles. These variables can be adjusted within the preset ranges, e.g., the drift length ranges from 0.1 to 2 m and the maximum strength of the quadrupoles is $30\,\mathrm{m}^{-2}$. Two objective functions are set to be: the weighted first order longitudinal dispersion α_1 and the weighted normalized CSR-induced emittance growth $\Delta\varepsilon_n$ obtained using the theoretical calculation formula of the CSR-kick model [15]. It is worth pointing out that, as the momentum compaction factor and the longitudinal dispersion functions can be related by $R_{56} = \alpha_1 z_0$, $T_{566} = \alpha_2 z_0$, and $U_{5666} = \alpha_3 z_0$, where z_0 is the trajectory length of reference particle which is a constant for a certain lattice. The matrix elements (R_{56}, T_{566} and U_{5666}) and momentum compaction factors (α_1, α_2 and α_3) are considered to be equivalent.

By imposing constraints, the optimization is conducted with practical considerations. For example, the horizontal and vertical beta functions are controlled to an acceptable range of 0.1 to 1000 m and the transverse dispersion function and its derivative as well as the chromaticity is corrected to zero. If anyone of the constraints is violated during the optimization process, the objective functions are multiplied by a factor lager than 1, which is referred to as the "weight factor". These weight factors are used to measure the quality of the objective functions to meet our optimization constrains.

Optimization of $\Delta\varepsilon_n$ and α_1

When the CSR induced emittance growth $\Delta\varepsilon_n$ and only the linear term α_1 are optimized, it is found that the second order term α_2 will become dominant as δ increases, as shown in Fig. 2, which is an example of the optimization. Despite that the CSR induced emittance growth and the linear term α_1 has been suppressed to an order of 10^{-9} and 10^{-11} respectively, the second order term α_2 grows rapidly and becomes dominant as δ increases. The relative longitudinal position variation of $\Delta z/z_0$ takes the shape of a parabola, which indicates that the second order term may be dominant in this case.
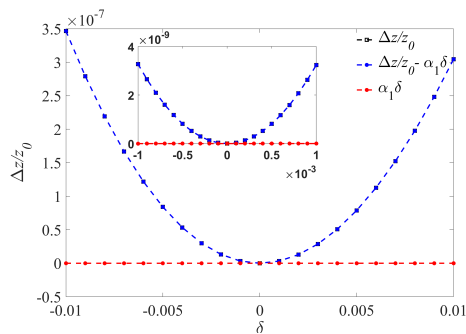

Figure 2: The relative longitudinal position variation w.r.t. the relative energy deviation δ of $[-10^{-2}, 10^{-2}]$ in the optimization case of $\Delta\varepsilon_n$ and α_1. The inset shows the δ range of $[-10^{-3}, 10^{-3}]$.

Optimization of $\Delta\varepsilon_n$ and α_1, α_2

The second and higher order longitudinal dispersion of the TBA are now of our concern. To mitigate the second order term α_2, we adopt a new weight factor in the optimization with the constraint that $|\alpha_1\delta| > 5|\alpha_2\delta^2|$, which is identified as our assumption that the linear term α_1 is dominant. With the adjusted constraints, the initial population evolves over 5000 generations. In the reign of $\alpha_1 < 10^{-7}$ and $\Delta\varepsilon_n < 10^{-8}$, one of the solutions is taken as an example. As can be seen in Fig. 3, when taking the second order term α_2 into consideration in the optimization, the residual of $\Delta z/z_0$ is flattened with δ ranging from -10^{-3} to 10^{-3}. However, as δ increases, the higher-order effects become evident and even dominate the longitudinal position variation, as shown in Fig. 3 when δ ranges from -10^{-2} to 10^{-2}.
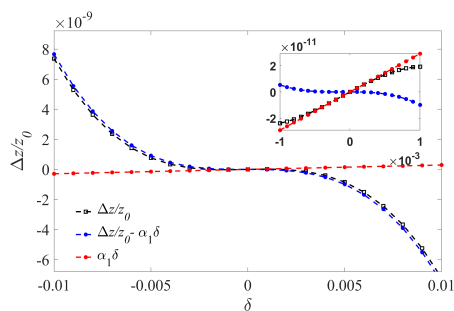

Figure 3: The relative longitudinal position variation w.r.t. the relative energy deviation δ of $[-10^{-2}, 10^{-2}]$ in the optimization case of $\Delta\varepsilon_n$ and α_1, α_2. The inset shows the δ range of $[-10^{-3}, 10^{-3}]$.

Optimization of $\Delta\varepsilon_n$ and α_1, Higher Order Terms

It is desirable for the isochronous TBA cell design if the residual high-order longitudinal dispersion functions, such as α_2, α_3 (or T_{566}, U_{5666}) and even higher orders, can be suppressed. A fully isochronous beam transport can be in demand, especially for the FEL injection line, which may need to accommodate a large beam energy spread [16]. These high order terms of longitudinal dispersion function can be investigated conveniently via numerical optimizations. Using adjusted weight factor, the case with δ ranging from -10^{-2} to 10^{-2} is optimized with the constraint that $|\alpha_1\delta| > 2|O(\delta^2)|$, in which $O(\delta^2)$ represents the terms of second order and above in the variable of δ, i.e., $O(\delta^2) = \Delta z/z - \alpha_1\delta$. We assume that the linear term α_1 is dominant if the constraint is satisfied. The initial population evolved over 5000 generations, and the results have become convergent, as can be seen in Fig. 4. The marked frontier solution is taken as an example, the results of which is shown in Fig. 5. The related parameters are shown in Table 1. It indicates that the higher orders are flattened compared with the linear term such that it enables linear transport of the high-brightness beams, i.e., the particles longitudinal position can be independent of δ.
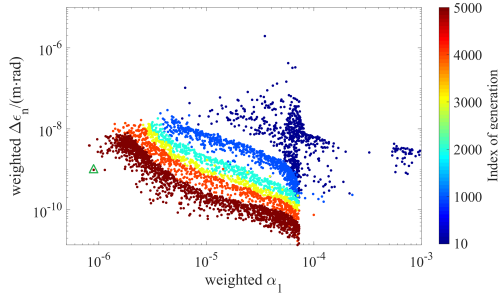
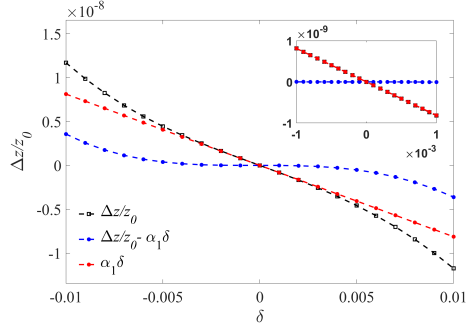Figure 4: Objective functions of the last 5000 generations.

Figure 5: The relative longitudinal position variation w.r.t. the relative energy deviation δ of $[-10^{-2}, 10^{-2}]$ in the optimization case of $\Delta\varepsilon_n$ and α_1, higher order terms. The inset shows the δ range of $[-10^{-3}, 10^{-3}]$.

COMPARISON OF THE TBA LENGTH

In practice, the overall length of the spreader system is expected to be fixed in advance. So, the length of our TBA design is fixed to a certain value, for example, 10 m in the optimization results mentioned above, for the convenience of meeting the requirements of different spreader design schemes flexibly. To further explore the potential of the design with a shorter length to achieve a compact scheme, different TBA designs with varying lengths are presented in this part. The CSR induced emittance growth and the linear term are optimized with the same constraint as using in the optimization case of $\Delta\varepsilon_n$ and α_1, higher order terms.

The solutions are shown in Figs. 6 and 7. It demonstrates that for the 8 m design, a set of solutions comparable with those of the 10 m and 15 m designs are found, which indicates that it is feasible to compress the TBA length to 8 m

Table 1: Values of the Optimization Result

Parameters	Value
α_1	8.952×10^{-7}
α_2	-4.615×10^{-6}
α_3	-0.0039
$O(\delta^2)(\delta = 10^{-3})$	8.489×10^{-12}
$O(\delta^2)(\delta = 10^{-2})$	4.128×10^{-9}
$\Delta\varepsilon_n(\text{m rad})$	9.078×10^{-10}

MC5: Beam Dynamics and EM Fields

D05 Coherent and Incoherent Instabilities - Theory, Simulations, Code Developments

with both $\Delta\varepsilon_n$ and α_1 minimized to the same scales as the 10 m and 15 m designs could do. It is worth pointing out that the results are obtained in the current parameters range. Comparable solutions may be found if the restrictions on variables are relaxed, which means it depends on the implementation of the hardware functionality.
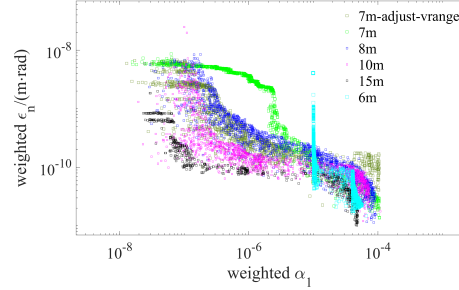

Figure 6: Results of different TBA lengths and the results with relative energy deviation δ ranging from -10^{-3} to 10^{-3}(hollow square).
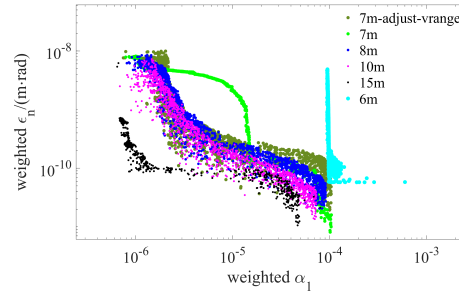

Figure 7: Results of different TBA lengths and the results with relative energy deviation δ ranging from -10^{-2} to 10^{-2}(solid dot).

CONCLUSION

In this study, by adopting MOPSO algorithm, TBA cell designs with stable optics that simultaneously minimize the CSR-induced emittance growth and the linear term R_{56}, the second order term T_{566} and higher order longitudinal dispersion are obtained. Such TBA design enables linear transport of the high-brightness beams, which is benefit for maintaining the high quality and can hopefully serve as a basic module in the beam transfer lines. The shortest possible beamline length of the higher-order isochronous TBA design is studied, which indicates that it is feasible to compress the TBA length to 8 m in the current parameter range. Our design strategy may be applied to the design of a cost-effective and compact FEL spreader.

REFERENCES

[1] Y. S. Derbenev, J. Rossbach, E. L. Saldin, and V. D. Shiltsev, "Microbunch radiative tail-head interaction", DESY, Hamburg, Germany, Rep. TESLA-FEL 95-05, Sep. 1995.

[2] S. Heifets and G. Stupakov, "Beam Instability and Microbunching due to Coherent Synchrotron Radiation", in *Proc.19th IEEE Particle Accelerator Conference (PAC 2001)*, Chicago, Illinois, 18-22 Jun 2001, paper TPPH081, pp.1856-1858.

[3] Z. Huang and K.-J. Kim, "Formulas for coherent synchrotron radiation microbunching in a bunch compressor chicane", *Phys. Rev. Accel. Beams*, vol. 5, p. 074401, Jul. 2002. `doi:10.1103/PhysRevSTAB.5.074401`

[4] M. Venturini, "Microbunching instability in single-pass systems using a direct two-dimensional Vlasov solver", *Phys. Rev. Accel. Beams*, vol. 10, p. 104401, Oct. 2007. `doi:10.1103/PhysRevSTAB.10.104401`

[5] C.-Y. Tsai, D. Douglas, R. Li, and C. Tennant, "Linear microbunching analysis for recirculation machines", *Phys. Rev. Accel. Beams*, vol. 19, p. 114401, Nov. 2016. `doi:10.1103/PhysRevAccelBeams.19.114401`

[6] C.-Y. Tsai, S. Di Mitri, D. Douglas, R. Li, and C. Tennant, "Conditions for coherent-synchrotron-radiation-induced microbunching suppression in multibend beam transport or recirculation arcs", *Phys. Rev. Accel. Beams*, vol. 20, p. 024401 Feb. 2017. `doi:10.1103/PhysRevAccelBeams.20.024401`

[7] C.-Y. Tsai, Ya. S. Derbenev, D. Douglas, R. Li, and C. Tennant, "Vlasov analysis of microbunching instability for magnetized beams", *Phys. Rev. Accel. Beams*, vol. 20, p. 054401, May. 2017. `doi:10.1103/PhysRevAccelBeams.20.054401`

[8] R.J. England, J.B. Rosenzweig, G. Andonian, P. Musumeci, G. Travish, and R. Yoder, "Sextupole correction of the longitudinal transport of relativistic beams in dispersionless translating sections", *Phys. Rev. ST Accel. Beams*, vol.8, p. 012801, Jan. 2005. `doi:10.1103/PhysRevSTAB.8.012801`

[9] C.-Y. Tsai, J. Wu, C. Yang, M. Yoon, and G. Zhou, "Sideband instability analysis based on a one-dimensional high-gain free electron laser model", *Phys. Rev. Accel. Beams*, vol. 20, p. 120702, Dec. 2017. `doi:10.1103/PhysRevAccelBeams.20.120702`

[10] C. A. Coello Coello and M. S. Lechuga, "MOPSO: a proposal for multiple objective particle swarm optimization", in *Proc. 2002 Congress on Evolutionary Computation (CEC'02)*, Honolulu, HI, USA, 12-17 May 2002, pp. 1051-1056. `doi:10.1109/CEC.2002.1004388`

[11] X. Pang and L.J. Rybarcyk, "Multi-objective particle swarm and genetic algorithm for the optimization of the LANSCE linac operation", *Nucl. Instrum. Methods Phys. Res., Sect. A*, vol. 741, pp. 124-129 Dec. 2014. `doi:10.1016/j.nima.2013.12.042`

[12] X. Huang and J. Safranek, "Nonlinear dynamics optimization with particle swarm and genetic algorithms for SPEAR3 emittance upgrade", *Nucl. Instrum. Methods Phys. Res., Sect. A*, vol. 757, pp. 48-53 Sep. 2014. `doi:10.1016/j.nima.2014.04.078`

[13] Y. Jiao and G. Xu, "Optimizing the lattice design of a diffraction-limited storage ring with a rational combination of particle swarm and genetic algorithms", *Chin. Phys. C*, vol. 41, no. 2, p.027001, 2017. `doi:10.1088/1674-1137/41/2/02700`

[14] J. Xu, P. Yang, G. Liu, Z. Bai, and W. Li, "Constraint handling in constrained optimization of a storage ring multi-bend-achromat lattice", *Nucl. Instrum. Methods Phys. Res., Sect. A*, vol. 988, p.164890, Nov. 2020. `doi:10.1016/j.nima.2020.164890`

[15] Y. Jiao, X. Cui, X. Huang, and G. Xu, "Generic conditions for suppressing the coherent synchrotron radiation induced emittance growth in a two-dipole achromat", *Phys. Rev. ST Accel. Beams*, vol. 17, p. 060701, Jun. 2014. `doi:10.1103/PhysRevSTAB.17.060701`

[16] W.A. Gillespie, "An FEL beam injection system with adjustable isochronism", *Nucl. Instrum. Methods Phys. Res., Sect. A* vol. 374, pp. 395-400, Jun. 1996. `doi:10.1016/0168-9002(96)00166-0`